ARMY RESEARCH LABORATORY

Mechanisms of Superplastic Deformation of Nanocrystalline Silicon Carbide Ceramics

by Yutaka Shinoda

ARL-CR-702 **August 2012**

NOTICES

Disclaimers

The findings in this report are not to be construed as an official Department of the Army position unless so designated by other authorized documents.

Citation of manufacturer's or trade names does not constitute an official endorsement or approval of the use thereof.

Destroy this report when it is no longer needed. Do not return it to the originator.

Army Research Laboratory
Aberdeen Proving Ground, MD 21005-5066

ARL-CR-702 **August 2012**

Mechanisms of Superplastic Deformation of Nanocrystalline Silicon Carbide Ceramics

Yutaka Shinoda
Tokyo Institute of Technology

REPORT DOCUMENTATION PAGE	Form Approved OMB No. 0704-0188

1. REPORT DATE *(DD-MM-YYYY)*	2. REPORT TYPE	3. DATES COVERED (From - To)
August 2012	Final	October 2008–September 2010

4. TITLE AND SUBTITLE
Mechanisms of Superplastic Deformation of Nanocrystalline Silicon Carbide Ceramics

5a. CONTRACT NUMBER
FA 5209-09-0272

5b. GRANT NUMBER

5c. PROGRAM ELEMENT NUMBER

6. AUTHOR(S)
Yutaka Shinoda

5d. PROJECT NUMBER
AH80

5e. TASK NUMBER

5f. WORK UNIT NUMBER

7. PERFORMING ORGANIZATION NAME(S) AND ADDRESS(ES)
Tokyo Institute of Technology
4259-R3-23
Nagatsuta-Cho
Midori-Ku
Yokohama 226-8503, Japan

8. PERFORMING ORGANIZATION REPORT NUMBER

9. SPONSORING/MONITORING AGENCY NAME(S) AND ADDRESS(ES)
U.S. Army Research Laboratory
ATTN: RDRL-WM
Aberdeen Proving Ground, MD 21005-5066

10. SPONSOR/MONITOR'S ACRONYM(S)

11. SPONSOR/MONITOR'S REPORT NUMBER(S)
ARL-CR-702

12. DISTRIBUTION/AVAILABILITY STATEMENT
Approved for public release; distribution is unlimited.

13. SUPPLEMENTARY NOTES

14. ABSTRACT

This project was undertaken to obtain preliminary data on the effect of nanograin size SiC materials on its properties. Using starting SiC powders with an average particle size of about 30 nm and small amounts of carbon and oxygen impurities, several processing techniques were used to fabricate bulk samples. These included the following: standard hot isostatic pressing (HIP), spark plasma sintering, ultra-high pressure HIP, and a multianvil pressure apparatus. The ultra-high pressure HIP technique achieved a final average grain size less than 100 nm and a relative percent of theoretical density of 96.8%; the hardness of this material was 22.7 GPa. A theoretical analysis of the effect of grain size on critical resolved shear stress to nucleate dislocations suggested a critical grain size of about 400 nm, below where it was easier to move partial dislocations. However, above this size, it was easier to move perfect dislocations. In addition, using more conventional hot-pressing techniques, the effect of different silicon and carbon contents was also investigated. It was found that increases in the free carbon and silicon content decreased the resulting grain size and influenced their strain rate sensitivity and flow stress.

15. SUBJECT TERMS
silicon carbide, nanostructure, sintering, hot isostatic pressing, hardness

16. SECURITY CLASSIFICATION OF:			17. LIMITATION OF ABSTRACT	18. NUMBER OF PAGES	19a. NAME OF RESPONSIBLE PERSON
a. REPORT	b. ABSTRACT	c. THIS PAGE			James W. McCauley
Unclassified	Unclassified	Unclassified	UU	22	19b. TELEPHONE NUMBER (*Include area code*) 410-306-0711

Standard Form 298 (Rev. 8/98)
Prescribed by ANSI Std. Z39.18

Contents

List of Figures

List of Tables

Foreword

This project has been co-funded by the U.S. Army International Technology Center - Pacific and the U.S. Army Research Laboratory (ARL) under the direction of Drs. J. W. McCauley and J. P. Singh of ARL.

1. Objective

The aim of the present study is to clarify the effect of the grain size and free-carbon content on the superplastic deformation in order to invent the high-performance nano-silicon carbide (SiC) ceramics and reveal the participation and morphology of dislocation activity in superplastic deformation of nano-SiC ceramics.

2. Results

2.1 Fabrication of Nanocrystalline SiC Ceramics

Nanocrystalline β-SiC powder with a mean particle size of 30 nm (Sumitomo-Osaka Cement Co., Tokyo, Japan, T-1 grade) was sintered without a sintering additive using several methods. The powder contained 3.7 weight-percent free carbon and 0.6 weight-percent impurity oxygen, and the amount of other metallic impurities was less than 1 ppm. Table 1 shows the characteristics of SiC sintered by various sintering methods. Figures 1–4 show the microstructure of the sintered SiC. The grain size decreased with decreasing sintering temperature. The grain size of the sintered body using multianvil apparatus was smallest; however, its hardness was extremely low in spite of relatively high density. The perfect bonding of SiC particles required a higher temperature than 1200 °C. The sintered body via the ultra-high pressure hot isostatic pressure (HIP) exhibited the highest density and highest hardness and fine grain size of less than 100 nm. The ultra-high pressure HIP was effective for fabricating high-quality nanocrystalline SiC ceramics.

Table 1. Characteristics of sintered SiC by various sintering methods.

Sintering Method	Sintering Conditions		Relative Density (%)	Hv (1 kgf) (kgf/mm^2)
	Temperature (C°)	Pressure (MPa)		
Standard HIP	2000	200	93.8	2000
Sinter forging by SPS	1800	500	93.5	2080
Ultra-high pressure HIP	1600	980	96.8	2270
Multianvil apparatus	1200	3000	94.8	1130

Note: SPS = spark plasma sintering.

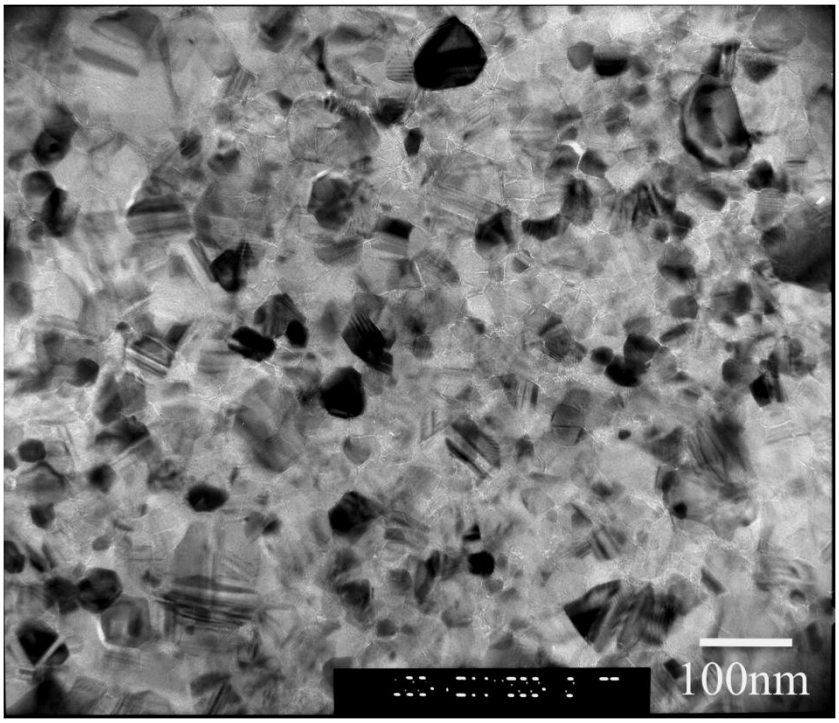

Figure 1. Ultra-high pressure HIP; 1600 °C, 980 MPa.

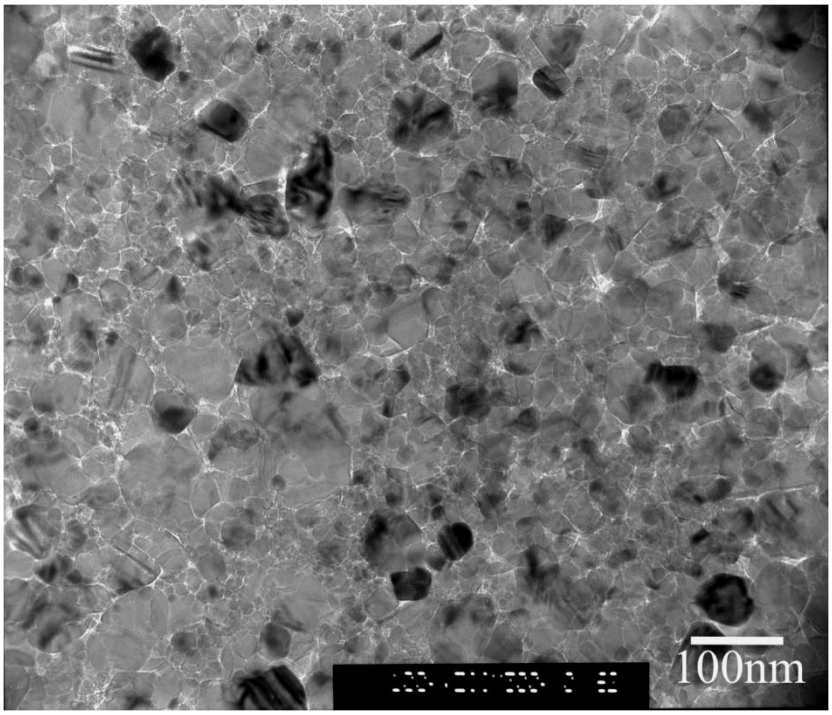

Figure 2. Multianvil high-pressure apparatus; 1200 °C, 3 GPa.

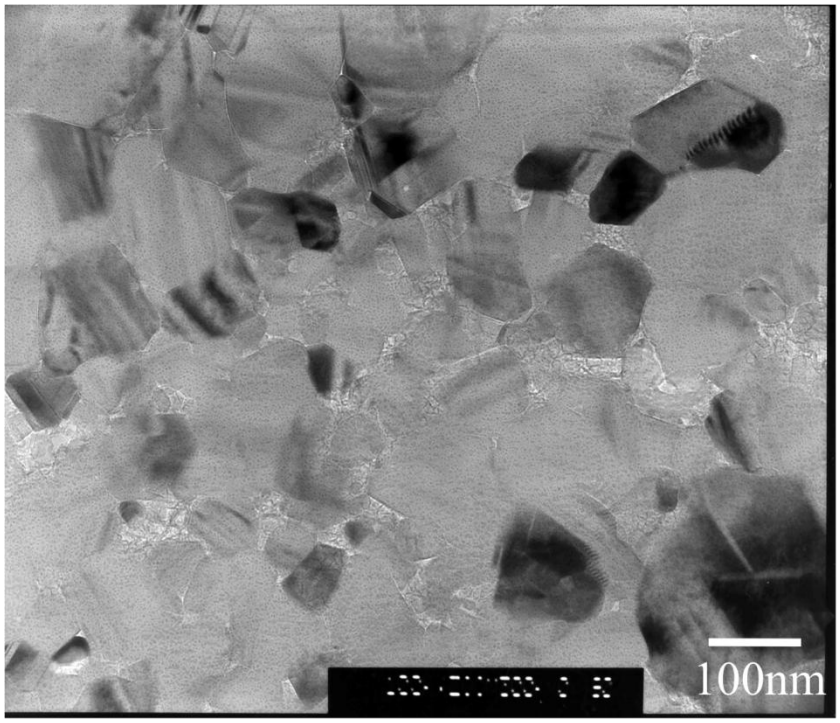

Figure 3. Standard HIP; 2000 °C, 200 MPa.

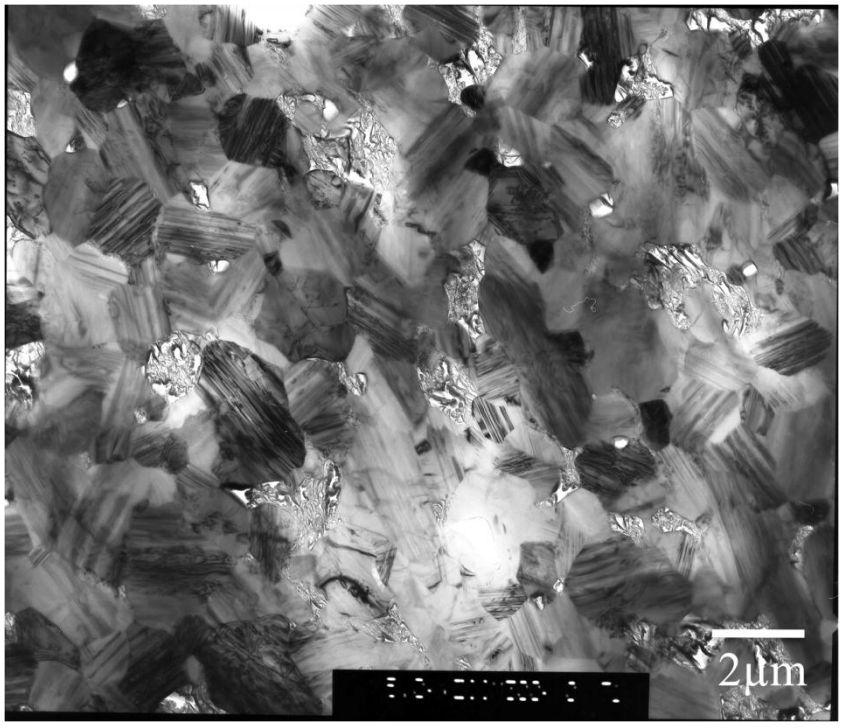

Figure 4. Sinter forging by SPS; 1800 °C, 500 MPa.

2.2 The Effect of the Grain Size on the Deformation at Elevated Temperature

The no-additive SiC ceramics with different grain sizes of 130 and 370 nm were prepared by annealing after HIPing. The strain rate ε˙0 at elevated temperature is expressed as a function of the applied stress σ and grain size d as

$$\dot{\varepsilon}_0 = A \frac{\sigma^n}{d^p} \exp\left(-\frac{Q}{kT}\right), \quad (1)$$

where n is the stress exponent, p is the grain size exponent, Q is the apparent activation energy for deformation, k is Boltzmann's constant, T is the temperature, and A is a constant. The stress exponent value was 2~3 and increased with decreasing strain rate. Such transition of stress exponent has been reported in superplastic zirconia ceramics and explained by the threshold model and/or the interface-controlled diffusion creep model. The origin of the transition of flow stress in SiC is currently unclear.

The flow stresses of SiC with smaller grain sizes were lower than those with larger grain sizes at a strain rate region of >1 × 10^{-5} s^{-1} (figure 5). On the other hand, at a strain rate region of <1 ×10^{-5} s^{-1}, the flow stresses of SiC with smaller grain sizes were higher than those with larger grain sizes. Generally, the flow stress increases with increasing grain size in the superplastic deformation region. In this region, the deformation rate is controlled by diffusion. A novel interpretation is required for the inverse grain-size dependence at a lower strain rate. It is possible that dislocation gliding is a possible mechanism of this deformation behavior of SiC.

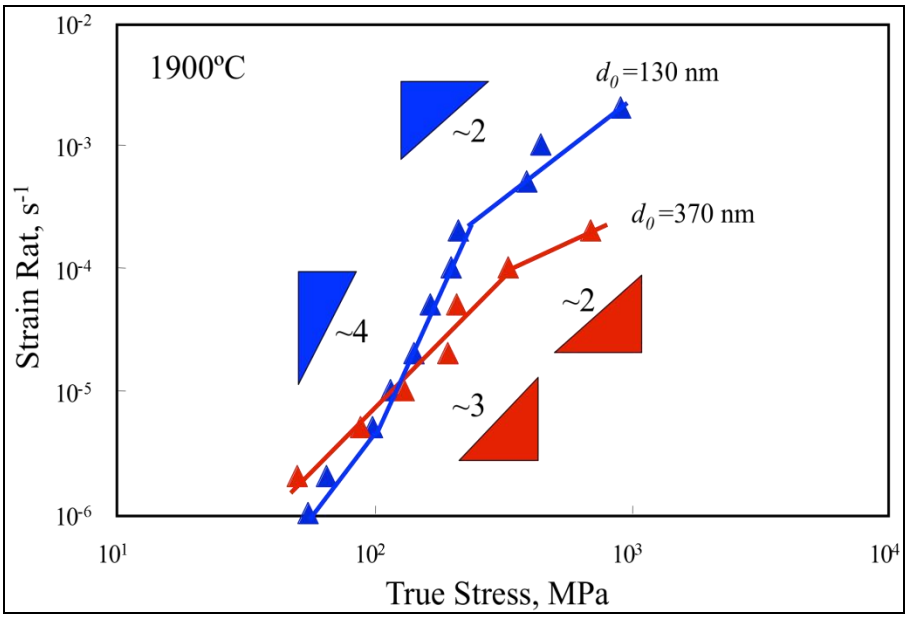

Figure 5. Relationship between stress and strain rate of SiC with different grain sizes.

2.3 Participation and Morphology of Dislocation Activity in Deformation of Nano-SiC Ceramics

Figure 6 indicates the relationship between grain size and calculated shear stress required for nucleation of dislocation in SiC. Because the shear modulus of SiC is very high, the critical shear stress is extremely high. This figure shows that a perfect dislocation was more easily nucleated than the partial dislocation in SiC with a larger grain size. On the other hand, the partial dislocation was more easily nucleated than a perfect dislocation in SiC with a smaller grain size. The critical grain size is ~400 nm. In both types of dislocations, the critical shear stress decreased with increasing grain size. The inverse grain-size dependence at the low stress region in figure 6 may relate to the dislocation activity as nucleation or gliding. Of course, the dominant mechanism of the nano-SiC is grain-boundary sliding. Moreover, the stress level to nucleate the dislocation was much higher than in the present experimental data. Therefore, dislocation gliding itself did not contribute to the total strain. It worked by accommodating stress concentration generated by the grain boundary sliding. If the grain size of nano-SiC were 130 nm, then the partial dislocation would be active.

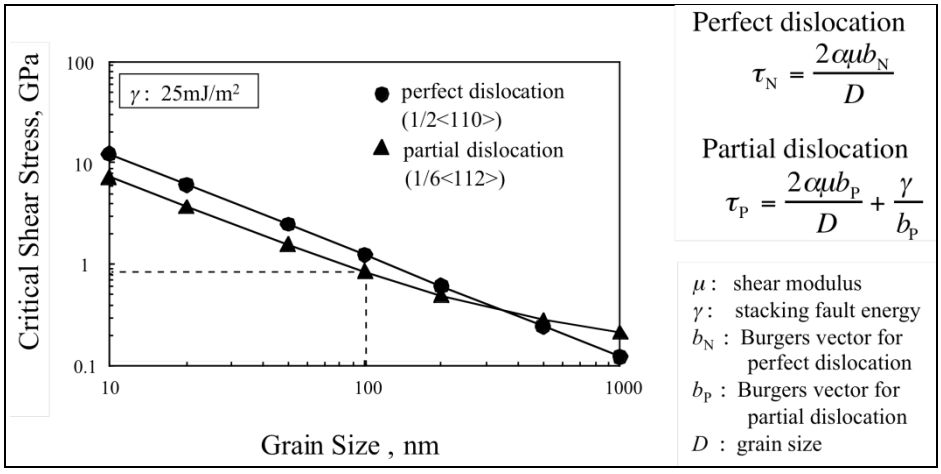

Figure 6. Relationship between grain size and shear stress required for nucleation of dislocation.

Figures 7–9 show transmission electron microscopy (TEM) micrographs of nano-SiC before and after deformation. After large deformation, the boundaries of the individual grains were not well defined and looked blurred, as in figure 2. The strain was stored in the grains. After annealing at 2100 °C, the stored strain seemed to disappear. The dislocations were hard to observe in SiC with the small grains. However, in SiC with the larger grains, they were often observed. We suspected that the movement of partial dislocations was important in the nano-SiC. Because the stacking fault energy of SiC was very low, it was reasonable for us to think that the partial dislocations moved through the nanograin, leaving the stacking faults.

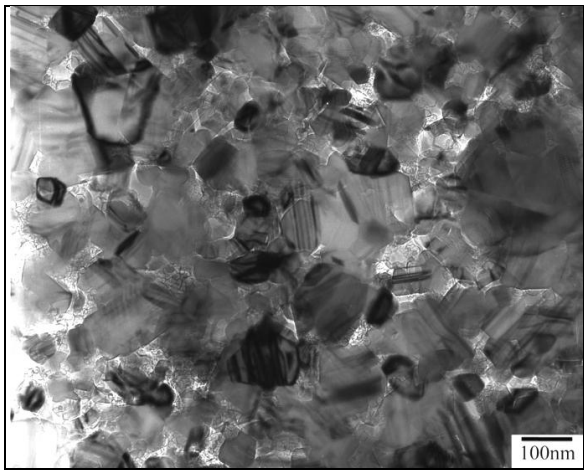

Figure 7. TEM image before deformation.

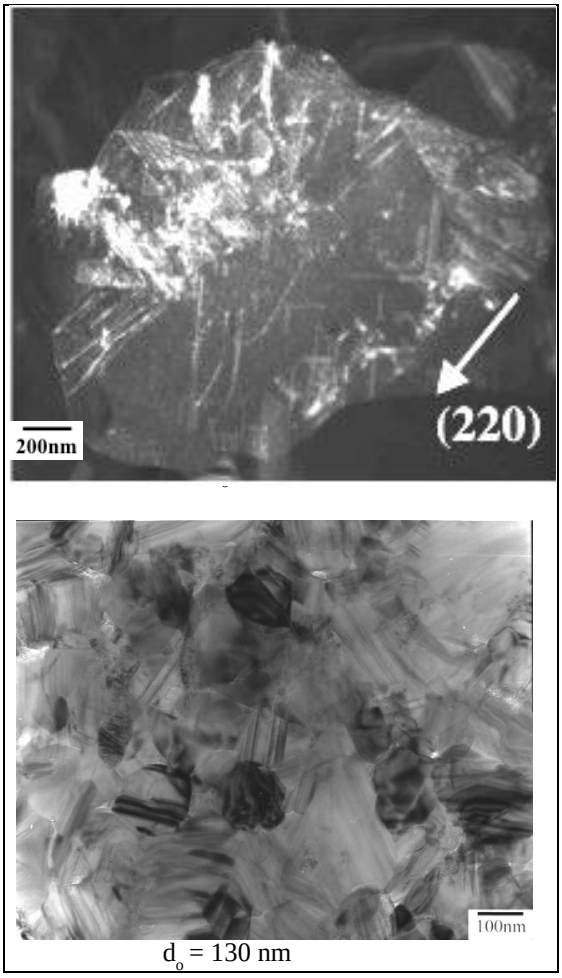

Figure 8. TEM image of deformed SiC
(1900 °C, 1×10^{-4} s^{-1}, $\varepsilon = 0.65$).

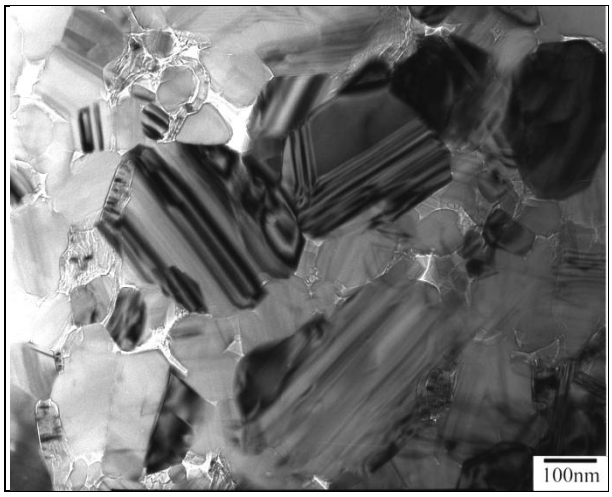

Figure 9. TEM image of annealed SiC (2100 °C, 1 h) after deformation.

2.4 The Effect of Carbon Content on the Deformation at Elevated Temperature

Nanosilicon powder was added to the β-SiC powder in order to control the carbon content. The mixed powder was sintered by hot-pressing to remove the impurity oxygen. The sintering was conducted at 2000 °C and 200 MPa using a SiC mold and SiC punches. The free carbon in SiC reacted with the impurity oxygen and added silicon as follows:

$$C(s) + SiO(g) \rightarrow SiC(s) + CO(g). \quad (2)$$

$$C(s) + Si(s) \rightarrow SiC(s). \quad (3)$$

Figure 10 shows SEM micrographs of hot-pressed SiC. The grain size of SiC decreased with increasing the carbon and silicon content. This suggested that the excess carbon and silicon segregated at the grain boundary, decreasing the grain-boundary diffusivity. Such an effect was contrary to boron and oxygen. Table 2 shows the characteristics of hot-pressed SiC. Figure 11 illustrates the relationship between the amount of excess silicon and carbon and grain size.

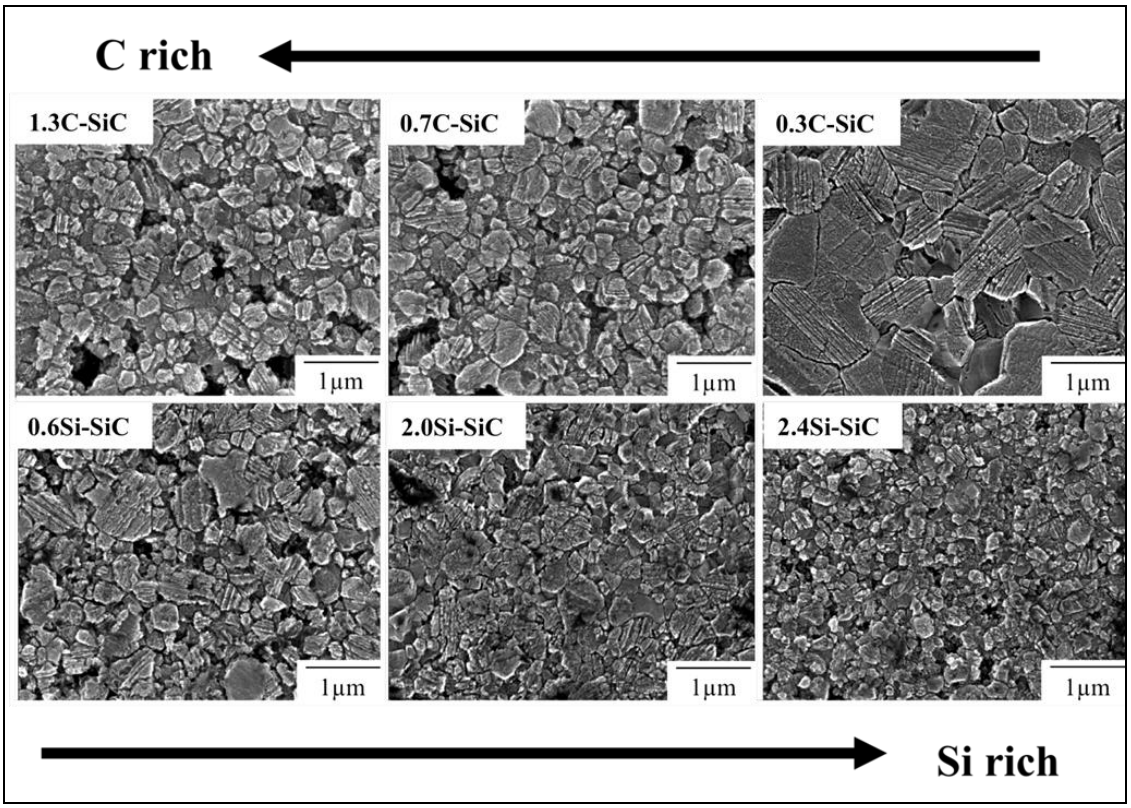

Figure 10. SEM micrographs of hot-pressed SiC.

Table 2. Hot-pressed SiC characteristics.

Designation	Excess Element (mol%)	Grain Size (nm)	Relative Density (%)
1.3C-SiC	1.3 (carbon)	350	95.5
0.7C-SiC	0.7 (carbon)	400	95.2
0.3C-SiC	0.3 (carbon)	760	98.9
0.6Si-SiC	0.6 (silicon)	470	97.4
2.0Si-SiC	2.0 (silicon)	400	98.1
2.4Si-SiC	2.4 (silicon)	270	97.9

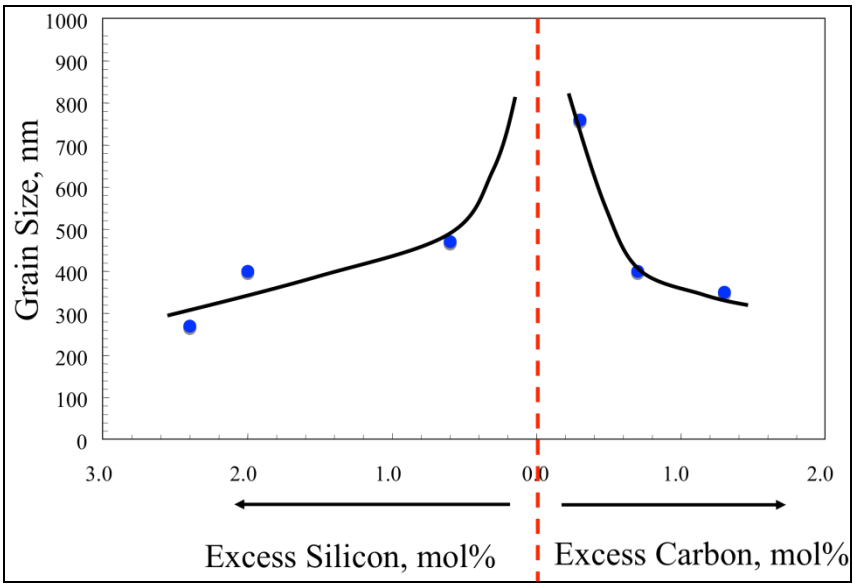

Figure 11. Relationship between the amount of excess carbon and silicon and grain size.

Figure 12 shows the relationship between the stress and strain rate in SiC with a different carbon and silicon content. The stress increased with increasing carbon content in spite of the decrease in grain size. The role of the excess carbon in SiC was quite the opposite of that of boron additive. The stress exponent tended to increase at a higher stress region. In this study, the effects of the excess carbon in pure SiC ceramics on the microstructure and deformation were revealed. The change of the structure and composition at the grain boundary by segregation of carbon atoms was interesting and will be researched in the future.

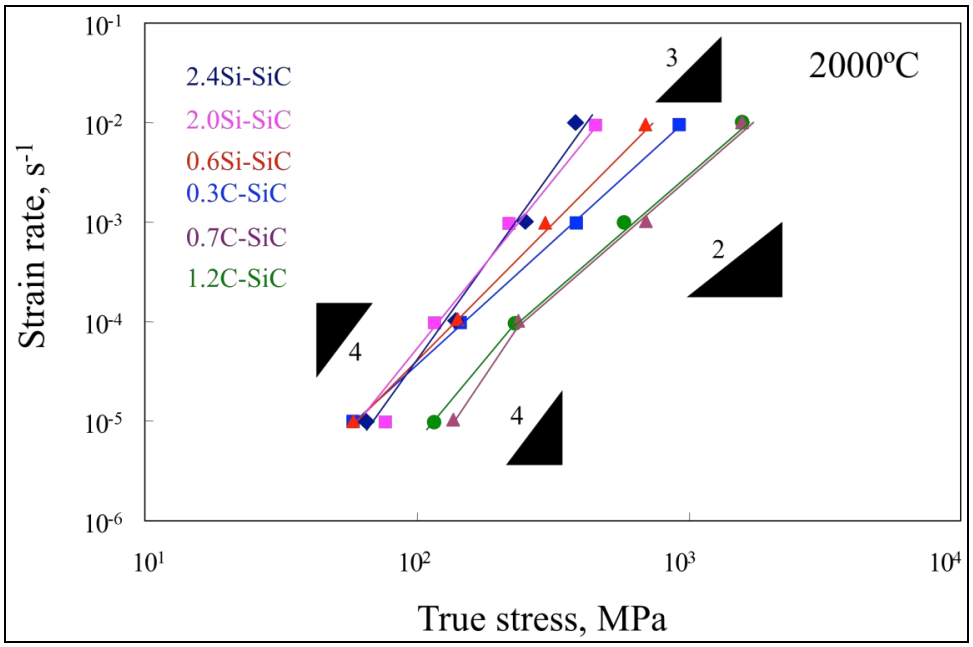

Figure 12. Relationship between stress and strain rate.

NO. OF COPIES	ORGANIZATION
1 (PDF only)	DEFENSE TECHNICAL INFORMATION CTR DTIC OCA 8725 JOHN J KINGMAN RD STE 0944 FORT BELVOIR VA 22060-6218
1	DIRECTOR US ARMY RESEARCH LAB IMAL HRA 2800 POWDER MILL RD ADELPHI MD 20783-1197
1	DIRECTOR US ARMY RESEARCH LAB RDRL CIO LL 2800 POWDER MILL RD ADELPHI MD 20783-1197

NO. OF COPIES ORGANIZATION

1 PEO GCS
SFAE GCS BCT/MS 325
M RYZYI
6501 ELEVEN MILE RD
WARREN MI 48397-5000

1 ABRAMS TESTING
SFAE GCSS W AB QT
J MORAN
6501 ELEVEN MILE RD
WARREN MI 48397-5000

1 COMMANDER
WATERVLIET ARSENAL
SMCWV QAE Q
B VANINA
BLDG 44
WATERVLIET NY 12189-4050

1 COMMANDER
US ARMY AMCOM
AVIATION APPLIED TECH DIR
J SCHUCK
FT EUSTIS VA 23604-5577

1 USA SBCCOM PM SOLDIER SPT
AMSSB PM RSS A
J CONNORS
KANSAS ST
NATICK MA 01760-5057

1 UNIV OF DELAWARE
DEPT OF MECH ENGR
J GILLESPIE
NEWARK DE 19716

3 AIR FORCE ARMAMENT LAB
AFATL DLJW
D BELK
J FOSTER
W COOK
EGLIN AFB FL 32542

1 TACOM ARDEC
AMSRD AAR AEE W
E BAKER
BLDG 3022
PICATINNY ARSENAL NJ
07806-5000

NO. OF COPIES ORGANIZATION

11 US ARMY TARDEC
AMSTRA TR R MS 263
K BISHNOI
D TEMPLETON (10 CPS)
WARREN MI 48397-5000

1 COMMANDER
US ARMY RSRCH OFC
A RAJENDRAN
PO BOX 12211
RSRCH TRIANGLE PARK NC
27709-2211

2 CALTECH
G RAVICHANDRAN
T AHRENS MS 252 21
1201 E CALIFORNIA BLVD
PASADENA CA 91125

5 SOUTHWEST RSRCH INST
C ANDERSON
K DANNEMANN
T HOLMQUIST
G JOHNSON
J WALKER
PO DRAWER 28510
SAN ANTONIO TX 78284

3 SRI INTERNATIONAL
D CURRAN
D SHOCKEY
R KLOOP
333 RAVENSWOOD AVE
MENLO PARK CA 94025 21

1 APPLIED RSRCH ASSOCIATES
D GRADY
4300 SAN MATEO BLVD NE
STE A220
ALBUQUERQUE NM 87110

1 INTERNATIONAL RSRCH
ASSOCIATES INC
D ORPHAL CAGE 06EXO
5274 BLACKBIRD DR
PLEASANTON CA 94566

1 BOB SKAGGS CONSULTANT
S R SKAGGS
7 CAMINO DE LOS GARDUNOS
SANTA FE NM 87506

NO. OF COPIES ORGANIZATION

2 WASHINGTON ST UNIV
INST OF SHOCK PHYSICS
Y GUPTA
J ASAY
PULLMAN WA 99164-2814

1 COORS CERAMIC CO
T RILEY
600 NINTH ST
GOLDEN CO 80401

1 UNIV OF DAYTON
RSRCH INST
N BRAR
300 COLLEGE PARK
MS SPC 1911
DAYTON OH 45469-0168

1 COMMANDER
US ARMY TACOM
AMSTA TR S
L PROKURAT FRANKS
WARREN MI 48397-5000

1 PM HBCT
SFAE GCS HBCT S
J ROWE MS 506
6501 11 MILE RD
WARREN MI 48397-5000

3 COMMANDER
US ARMY RSRCH OFC
B LAMATINA
D STEPP
W MULLINS
PO BOX 12211
RSRCH TRIANGLE PARK NC
27709-2211

1 NAVAL SURFACE WARFARE CTR
CARDEROCK DIVISION
R PETERSON
CODE 28
9500 MACARTHUR BLVD
WEST BETHESDA MD 20817-5700

2 LAWRENCE LIVERMORE NATL LAB
R LANDINGHAM L369
J E REAUGH L282
PO BOX 808
LIVERMORE CA 94550

NO. OF COPIES ORGANIZATION

3 SANDIA NATL LAB
J ASAY MS 0548
L CHHABILDAS MS 0821
D CRAWFORD ORG 0821
PO BOX 5800
ALBUQUERQUE NM 87185-0820

1 RUTGERS
THE STATE UNIV OF NEW JERSEY
DEPT OF CRMCS & MATLS ENGRNG
R HABER
607 TAYLOR RD
PICATINNY NJ 08854

1 THE UNIVERSITY OF TEXAS
AT AUSTIN
S BLESS
IAT
3925 W BRAKER LN STE 400
AUSTIN TX 78759-5316

1 CERCOM
R PALICKA
1960 WATSON WAY
VISTA CA 92083

6 GDLS
W BURKE MZ436 21 24
G CAMPBELL MZ436 30 44
D DEBUSSCHER MZ436 20 29
J ERIDON MZ436 21 24
W HERMAN MZ435 01 24
S PENTESCU MZ436 21 24
38500 MOUND RD
STERLING HTS MI 48310-3200

1 JET PROPULSION LAB
IMPACT PHYSICS GROUP
M ADAMS
4800 OAK GROVE DR
PASADENA CA 91109-8099

3 OGARA HESS & EISENHARDT
G ALLEN
D MALONE
T RUSSELL
9113 LE SAINT DR
FAIRFIELD OH 45014

NO. OF COPIES	ORGANIZATION
1	CERADYNE INC M NORMANDIA 3169 REDHILL AVE COSTA MESA CA 96626
2	JOHNS HOPKINS UNIV DEPT OF MECH ENGRNG K T RAMESH T W WRIGHT 3400 CHARLES ST BALTIMORE MD 21218
2	SIMULA INC V HORVATICH V KELSEY 10016 51ST ST PHOENIX AZ 85044
3	UNITED DEFENSE LP K STRITTMATTER E BRADY R JENKINS PO BOX 15512 YORK PA 17405-1512
10	NATL INST OF STANDARDS & TECH CRMCS DIV G QUINN STOP 852 GAITHERSBURG MD 20899
2	DIR USARL RDRL D C CHABALOWSKI V WEISS 2800 POWDER MILL RD ADELPHI MD 20783-1197 23
	ABERDEEN PROVING GROUND
60	DIR USARL RDRL SL R COATES RDRL WM S KARNA P BAKER J MCCAULEY (10 CPS) RDRL WML J NEWILL M ZOLTOSKI RDRL WML B D TAYLOR (10 CPS) RDRL WMM R DOWDING

NO. OF COPIES	ORGANIZATION
	RDRL WMM A J SANDS T WEERASOORIYA RDRL WMM D E CHIN K CHO G GAZONAS R SQUILLACIOTI RDRL WMM E J LASALVIA P PATEL RDRL WMM F J MONTGOMERY RDRL WMP B BURNS S SCHOENFELD RDRL WMP B C HOPPEL M SCHEIDLER RDRL WMP C T BJERKE J CLAYTON D DANDEKAR M GREENFIELD S SEGLETES W WALTERS RDRL WMP D T HAVEL M KEELE D KLEPONIS H MEYER J RUNYEON RDRL WMP E P BARTKOWSKI M BURKINS W GOOCH D HACKBARTH E HORWATH T JONES RDRL WML H T FARRAND L MAGNESS D SCHEFFLER R SUMMERS

INTENTIONALLY LEFT BLANK.